

Excitation of the Isovector Spin Monopole Resonance via the Exothermic $^{90}\text{Zr}(^{12}\text{N}, ^{12}\text{C})$ Reaction at 175 MeV/ u

S. Noji,^{1,2,*} H. Sakai,^{1,3} N. Aoi,^{3,†} H. Baba,³ G. P. A. Berg,^{4,5} P. Doornenbal,³ M. Dozono,^{3,‡} N. Fukuda,³ N. Inabe,³ D. Kameda,³ T. Kawabata,⁶ S. Kawase,^{2,§} Y. Kikuchi,² K. Kisamori,² T. Kubo,^{3,||} Y. Maeda,⁷ H. Matsubara,^{2,¶} S. Michimasa,² K. Miki,^{1,**} H. Miya,² H. Miyasako,⁷ S. Sakaguchi,⁸ Y. Sasamoto,² S. Shimoura,² M. Takaki,² H. Takeda,³ S. Takeuchi,³ H. Tokieda,² T. Ohnishi,³ S. Ota,² T. Uesaka,^{2,††} H. Wang,³ K. Yako,^{1,‡‡} Y. Yanagisawa,³ N. Yokota,⁶ K. Yoshida,³ and R. G. T. Zegers^{9,5,10}

¹Department of Physics, University of Tokyo, Hongo, Bunkyo, Tokyo 113-0033, Japan

²Center for Nuclear Study, University of Tokyo, RIKEN Campus, Wako, Saitama 351-0198, Japan

³RIKEN Nishina Center, Hirosawa, Wako, Saitama 351-0198, Japan

⁴Department of Physics, University of Notre Dame, Nieuwland Science Hall, Notre Dame, Indiana 46556, USA

⁵The JINA Center for the Evolution of the Elements, Michigan State University, East Lansing, Michigan 48824, USA


⁶Department of Physics, Kyoto University, Kitashirakawa, Oiwakecho, Sakyo, Kyoto 606-8502, Japan

⁷Department of Applied Physics, University of Miyazaki, Miyazaki, Miyazaki 889-2192, Japan

⁸Department of Physics, Kyushu University, Nishi, Fukuoka 819-0395, Japan

⁹National Superconducting Cyclotron Laboratory, Michigan State University, East Lansing, Michigan 48824, USA

¹⁰Department of Physics and Astronomy, Michigan State University, East Lansing, Michigan 48824, USA

 (Received 30 January 2018; revised manuscript received 9 March 2018; published 26 April 2018)

The (^{12}N , ^{12}C) charge-exchange reaction at 175 MeV/ u was developed as a novel probe for studying the isovector spin giant monopole resonance (IVSMR), whose properties are important for better understanding the bulk properties of nuclei and asymmetric nuclear matter. This probe, now available through the production of ^{12}N as a secondary rare-isotope beam, is exothermic, is strongly absorbed at the surface of the target nucleus, and provides selectivity for spin-transfer excitations. All three properties enhance the excitation of the IVSMR compared to other, primarily light-ion, probes, which have been used to study the IVSMR thus far. The $^{90}\text{Zr}(^{12}\text{N}, ^{12}\text{C})$ reaction was measured and the excitation energy spectra up to about 70 MeV for both the spin-transfer and non-spin-transfer channels were deduced separately by tagging the decay by γ emission from the ^{12}C ejectile. Besides the well-known Gamow-Teller and isobaric analog transitions, a clear signature of the IVSMR was identified. By comparing with the results from light-ion reactions on the same target nucleus and theoretical predictions, the suitability of this new probe for studying the IVSMR was confirmed.

DOI: [10.1103/PhysRevLett.120.172501](https://doi.org/10.1103/PhysRevLett.120.172501)

The study of giant resonances provides information about the bulk properties of atomic nuclei and the nuclear response at high excitation energies [1]. Inspired by the successful investigation of the isoscalar giant monopole resonance, which has yielded important information about the incompressibility of nuclear matter [2–4], significant efforts have been made to gain a better understanding of the properties of its isovector partners, the isovector giant monopole resonance (IVGMR) and the isovector spin giant monopole resonance (IVSMR). Their characteristics provide additional insight into the bulk properties of nuclei and nuclear matter. The IVGMR and the IVSMR are both breathing modes in which the proton and neutron density distributions oscillate out of phase. In the case of the IVSMR, which is the focus of the present Letter, the excitation is additionally associated with the transfer of spin [5,6]. The properties of these monopole resonances are sensitive to the surface and volume symmetry-energy

coefficients [7], and a systematic study over a wide range of target masses provides a complementary method to other techniques to constrain these quantities, which are key for understanding the properties of asymmetric nuclear matter, including neutron stars [8]. Furthermore, the non-energy-weighted sum rule (NEWSR) for the IVSMR is connected to the proton and neutron distributions in nuclei as $S_- - S_+ = 3[N\langle r^4 \rangle_n - Z\langle r^4 \rangle_p]$, where S_- (S_+) is the IVSMR transition strength associated with the transition strength in the β^- (β^+) directions. Therefore, high-quality data on the IVSMR would provide a sensitive measure of the neutron-skin thickness, $\delta_{np} = \sqrt[4]{\langle r^4 \rangle_n} - \sqrt[4]{\langle r^4 \rangle_p}$, from which the density dependence of the symmetry energy for asymmetric nuclear matter can be constrained [9,10]. Detailed knowledge about the nuclear spin-isospin responses up to high excitation energies, including that about the IVSMR, can have a significant

impact on, e.g., modeling astrophysically important weak-interaction processes and characterizing neutrino-nucleus reactions [11,12].

Experimental studies of the IVSMR are challenging. In a microscopic picture, it is a coherent $2\hbar\omega 1p\text{-}1h$ transition with $\Delta L = 0$ and $\Delta S = \Delta T = 1$, driven by an operator $\hat{O}_{\pm} = \sum_k t_{\pm}(k)\sigma_{\mu}(k)r(k)^2$, where t_{\pm} is the raising or lowering isospin operator and σ_{μ} is the μ -component spin operator, respectively [5,6]. The excitation energy of the IVSMR is high (20–50 MeV) and the resonance broad ($\Gamma \sim 10$ MeV). Evidence for the existence of the IVSMR in the β^- direction comes from the (p, n) reaction at 800 MeV [13] and $({}^3\text{He}, t)$ experiments [14–16]. In the β^+ direction, where the excitation energy of the IVSMR is lower than in the β^- direction, very promising results have been obtained by using the $(t, {}^3\text{He})$ reaction [17–19].

Here, we present an innovative spectroscopic tool, the $({}^{12}\text{N}, {}^{12}\text{C})$ reaction at 175 MeV/ u , which is used to excite the IVSMR from a ${}^{90}\text{Zr}$ target. The $({}^{12}\text{N}, {}^{12}\text{C})$ reaction, with an unstable ${}^{12}\text{N}$ beam, has three preminent advantages for studying the IVSMR. First, it has a large positive ground-state (g.s.) mass difference of 16.83 MeV between the projectile and the ejectile. Therefore, the reaction is exothermic up to relatively high values of energy transfer (ω) to the target nucleus and, as shown in Fig. 1, associated with small linear momentum transfer q ($\lesssim 0.34$ fm $^{-1}$) for $\omega \lesssim 50$ MeV, the energy region of the IVSMR. A recoilless condition ($q = 0$) is achieved at $\omega \simeq 14$ MeV. This feature is very beneficial for exciting the $\Delta L = 0$ IVSMR and cannot be achieved with stable-ion probes. Second, due to the strong absorption, this heavy-ion-induced reaction probes only the surface region of the transition density. The transition density of the IVSMR has a node near the nuclear surface, and the strong absorption ensures that no cancellation between the inner and surface regions of the

transition densities occurs, in contrast to the (p, n) reaction [20,21] at beam energies near 200 MeV. Finally, in a reaction from the $J^{\pi} = 1^+, T = 1, {}^{12}\text{N}(\text{g.s.})$ to the $J^{\pi} = 0^+, T = 0, {}^{12}\text{C}(\text{g.s.})$, $\Delta S = \Delta T = 1$ is guaranteed and the reaction exclusively excites spin- and isospin-transfer modes, including the Gamow-Teller (GT, $0\hbar\omega$, $\Delta L = 0$, and $\Delta S = \Delta T = 1$) and IVSMR resonances (see Ref. [22] for more details on angular momentum transfer). Such selectivity is not achieved for the (p, n) or $({}^3\text{He}, t)$ reactions, for which the projectile and the ejectile both have $J^{\pi} = 1/2^+$ and $T = 1/2$, where both $\Delta S = 0$ and $\Delta S = 1$ modes can be excited, and preference for spin-transfer excitations can only be achieved by optimizing the incident beam energy, because the ratio of the $\sigma\tau$ (spin-transfer) and τ (non-spin-transfer) components of the effective NN interaction takes a maximum value at around 300 MeV [23–25].

The $({}^{12}\text{N}, {}^{12}\text{C})$ reaction is studied by measuring the ${}^{12}\text{C}$ ejectile. If the ${}^{12}\text{C}$ ejectile is produced in an excited state that decays by γ emission, instead of the ground state, the selectivity described above is partially lost. The contribution to the total cross section from transitions to the only bound state at 4.4 MeV below the α -decay threshold is relatively small, because the $\log ft$ value of 5.1 for the transition from ${}^{12}\text{N}$ to the 4.4-MeV state in ${}^{12}\text{C}$ is much larger than the value of 4.1 for that to the ground state. However, the transition to the 1^+ state at 15.1 MeV in ${}^{12}\text{C}$ ($J^{\pi} = 1^+, T = 1$) is a superallowed Fermi transition, and the contribution is stronger. Since its decay by particle emission is isospin forbidden, this state decays directly to the ${}^{12}\text{C}$ ground state by γ emission, and the contribution of this transition can be evaluated by detecting the deexcitation γ ray with an energy of 15.1 MeV in coincidence with ${}^{12}\text{C}$. Studying this decay offers a possibility to gain selectivity for Fermi-type $\Delta S = 0, \Delta T = 1$ transitions, in addition to the aforementioned selectivity offered for GT-type $\Delta S = 1, \Delta T = 1$ transitions. (Hereafter, these transitions are, respectively, referred to as the Fermi and GT channels).

In the present study, ${}^{90}\text{Zr}$ was selected as reaction target because the GT giant resonance (GTGR) and the isobaric analog state (IAS) have been extensively studied, and signatures of the IVSMR in the β^- direction have been reported [13,14,26].

A 250-MeV/ u , 400-pnA beam of ${}^{14}\text{N}$ was impinged upon a 5-mm-thick beryllium target, and ${}^{12}\text{N}$ nuclei were selected among the various projectile fragments in the BigRIPS fragment separator [27]. To achieve high purity of ${}^{12}\text{N}$, a 15-mm-thick wedge-shaped aluminum degrader was used. The ${}^{12}\text{N}$ beam (with a rate of 1.8 Mpps, purity of 92%, and average energy of 175 MeV/ u) was transported to the ${}^{90}\text{Zr}$ reaction target using the dispersion-matching technique [28]. The incoming beam trajectories were measured with two low-pressure multiwire drift chambers [29]

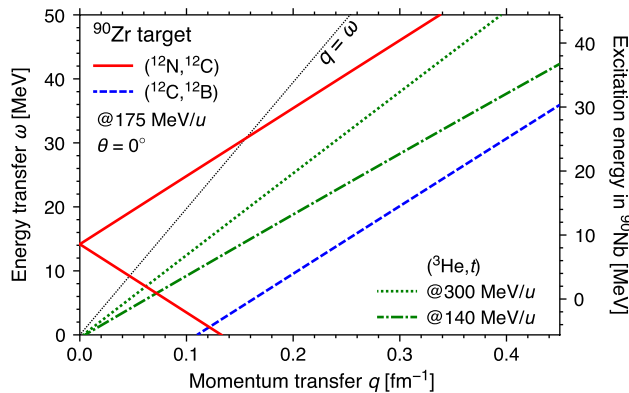


FIG. 1. Two-body reaction kinematics on the q - ω plane, showing the exothermic nature of the $({}^{12}\text{N}, {}^{12}\text{C})$ reaction and the low linear momentum transfer in comparison with other probes. The excitation energy (E_x) in ${}^{90}\text{Nb}$ is shown on the right, with $E_x = \omega + \Delta m$, where $\Delta m = 5.60$ MeV is the ground-state mass difference between ${}^{90}\text{Nb}$ and ${}^{90}\text{Zr}$.

installed 1 m upstream of the target. The ^{90}Zr target (99.4% isotopic enrichment) was 154-mg/cm^2 thick, with a dimension of 80 mm (in the dispersive direction) by 30 mm (nondispersive).

The ^{12}C ejectiles were analyzed by the SHARAQ spectrometer [30], and their trajectories were measured with two cathode-readout drift chambers placed at the focal plane. Scattering angles and momenta of the outgoing ^{12}C were reconstructed on an event-by-event basis. Three plastic scintillators (5-, 10-, and 20-mm thick) at the focal plane enabled particle identification through a combination of energy-loss and time-of-flight measurements. The excitation energy in ^{90}Nb was obtained in a missing-mass calculation over the range $0 \leq E_x \lesssim 70$ MeV with a resolution of 8 MeV, which was due to a contribution from the intrinsic resolution of 4.6 MeV (FWHM) of the reconstruction, as estimated from the observed $^{12}\text{N}^{6+}$ charge-state peak and a contribution from the difference in the energy losses of 6 MeV in the ^{90}Zr target between ^{12}N and ^{12}C . Scattering angles were measured over the range $0^\circ \leq \theta_{\text{c.m.}} \lesssim 3^\circ$ with a resolution of 0.6° (FWHM).

The NaI(Tl) scintillator array DALI2 [31], installed surrounding the target, was used for tagging deexcitation γ rays from ^{12}C . The highly granulated DALI2 array allowed the determination of the emission angles of γ rays, which were used in the Doppler reconstruction of their energies. In order to determine the contribution from the γ rays emitted from the 15.1-MeV state in ^{12}C , all γ rays with a Doppler-reconstructed γ -ray energy above 8 MeV were selected, since the majority of the 15.1-MeV γ rays do not deposit all of their energy in the detector and relatively few γ rays with energies above 8 MeV are emitted from the ^{90}Nb residual nucleus [as observed in the $^{90}\text{Zr}(^3\text{He}, t + \gamma)$ reaction at 150 MeV/u [32]]. The detection efficiency for the 15.1-MeV γ rays was estimated to be $38 \pm 5\%$ by a GEANT4 simulation. The 4.4-MeV γ ray from the 2_1^+ state was also observed, but the subtraction of this contribution by the γ -ray tagging technique was a challenge because of the large number of γ rays with similar energies from ^{90}Nb in this energy region. Since this excitation is also of spin-transfer nature and an order of magnitude smaller than the transition to the $^{12}\text{C}(\text{g.s.})$, and the shift in excitation energy is smaller than the excitation-energy resolution, its contribution to the final spin-transfer spectrum was not subtracted.

^{12}N beam particles can β decay in flight (half-life of 11.0 ms [33]) to ^{12}C near the target and contribute to the background in the data, and its contribution is roughly 2 orders of magnitude larger than that of the charge-exchange reaction products. It was eliminated by measuring the energy loss in two 1-mm-thick plastic scintillators, installed at a distance of 8 mm upstream and downstream of the ^{90}Zr target. Only events that were identified as ^{12}N prior to the target and ^{12}C after the target were selected for the remainder of the analysis. With this scintillator cut, the

contribution of the in-flight β decay was suppressed by a factor of about 10^3 . Contributions due to the reactions that took place in these scintillators were evaluated by removing the ^{90}Zr target. The number of these events was approximately equal to the true events induced by the ^{90}Zr target, and these background events were subtracted from the spectrum. It should be noted that the ^{12}C from the in-flight β decay is located in the excitation-energy spectrum below ~ 10 MeV and does not contribute to the uncertainties in the discussion of the properties of the IVSMR below.

The double-differential cross-section spectra for the GT channel are shown in Fig. 2(a). Two broad peaks are seen at around $E_x \approx 10$ and $E_x = 20\text{--}50$ MeV in the $0^\circ\text{--}1^\circ$ spectrum, which are no longer visible at the larger scattering angles, indicative of monopole transitions. By comparison with results from previous β^- charge-exchange experiments, such as in Ref. [26], the lower peak is identified as the GTGR. The systematic uncertainties in the absolute cross sections are estimated to be about $\pm 20\%$ and are dominated by the uncertainties in the number of incoming beam particles and in the background-subtraction procedures. The double-differential cross-section spectra for the Fermi channel are shown in Fig. 2(b). A clear peak

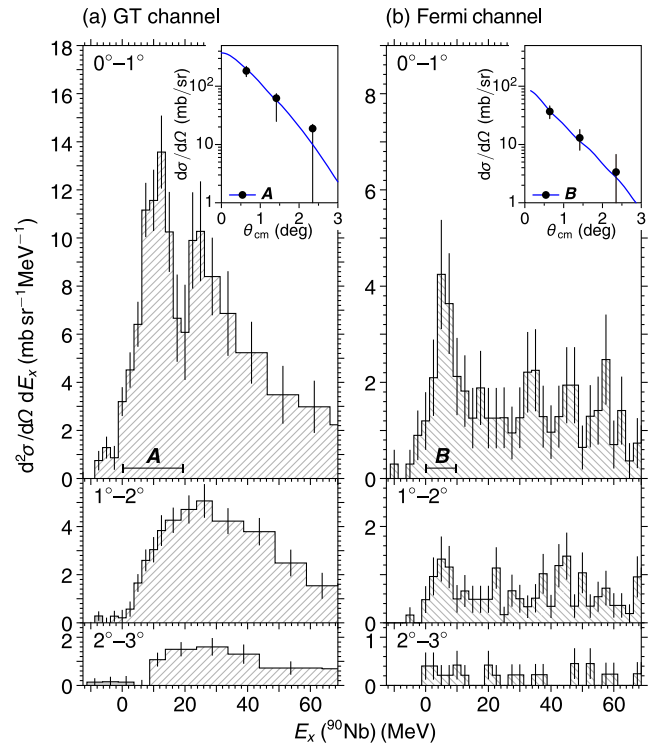


FIG. 2. (a) Double-differential cross sections for the GT channel. The error bars denote only statistical uncertainties. The inset shows the angular distribution of the cross sections for the peak in the energy range A and is compared with a DWBA calculation for the GTGR. (b) *Idem*, but for the Fermi channel. The inset shows the angular distribution for the peak in the energy range B and is compared with DWBA for the IAS.

at $E_x \approx 5$ MeV was observed, consistent with the known excitation energy of the IAS in ^{90}Nb [26].

The angular distributions of the cross sections for the peaks in energy ranges *A* (GT) and *B* (Fermi) are shown in the insets of Fig. 2. These are obtained by integrating the cross sections in the relevant energy ranges. They are compared with calculations in the distorted-wave Born approximation (DWBA), which were performed using the microscopic double-folding code FOLD/DWHI [34]. One-body transition densities for the ^{12}N - ^{12}C system were calculated in the *psd*-shell-model space with the SFO (Suzuki-Fujimoto-Otsuka) interaction [35] in NUSHELLX@MSU [36], while those for the ^{90}Zr - ^{90}Nb system were calculated in the normal-modes (NMs) formalism [37]. The NMs calculation exhausts 100% of the NEWSR associated with the IVSMR operator (10387 fm^4). The Franey-Love effective *NN* interaction at 175 MeV [24] was used. The optical-model-potential parameters (OMPs) for the entrance ($^{12}\text{N} + ^{90}\text{Zr}$) and the exit ($^{12}\text{C} + ^{90}\text{Nb}$) channels were obtained through the double-folding-model procedure with a complex Gaussian-parametrized *G* matrix *NN* interaction CEG07b [38–41] and the density distribution of Ref. [42].

For the GT (Fermi) channel, the forward-peaked angular distribution of the cross sections in the range *A* (*B*) agrees well with the DWBA cross sections for the GTGR (IAS). No significant contributions from other multipoles were found in these energy ranges. The scaling factor required to match the calculated differential cross sections with those observed (primarily arising from uncertainties in the OMPs) was also applied to the comparison of the IVSMR cross sections discussed below.

In order to gain insight into the nature of the broad peak observed at $E_x = 20$ – 50 MeV in the GT channel shown in Fig. 2(a), the excitation-energy spectrum was compared with those of the (*p*, *n*) reaction at 795 MeV [13] and 200 MeV [43], and the (^3He , *t*) reaction at 300 MeV/*u* [14], as shown in Fig. 3(a). The previous data were smeared to match the resolution of the present data and scaled such that the GTGR peaks coincide. Since the excitation of the IVSMR is strongly reduced in the (*p*, *n*) reaction at 200 MeV, due to the cancellation of the inner and surface components of the transitions amplitudes as discussed above, it was used to subtract from the (^{12}N , ^{12}C), the (*p*, *n*) spectrum at 795 MeV and the (^3He , *t*) spectrum at 300 MeV/*u*, as shown in Fig. 3(b). The excitation of the IVSMR is enhanced in the excitation-energy region below 30 MeV relative to the spectra from these other two reactions, indicating that the (^{12}N , ^{12}C) reaction is indeed a powerful tool for the investigation of the IVSMR.

The extracted strength distribution for the IVSMR, which was obtained by dividing the cross-section difference by the excitation-energy-dependent DWBA calculation for the IVSMR with NMs input strengths, is shown in Fig. 3(c). The strength extracted at high E_x is

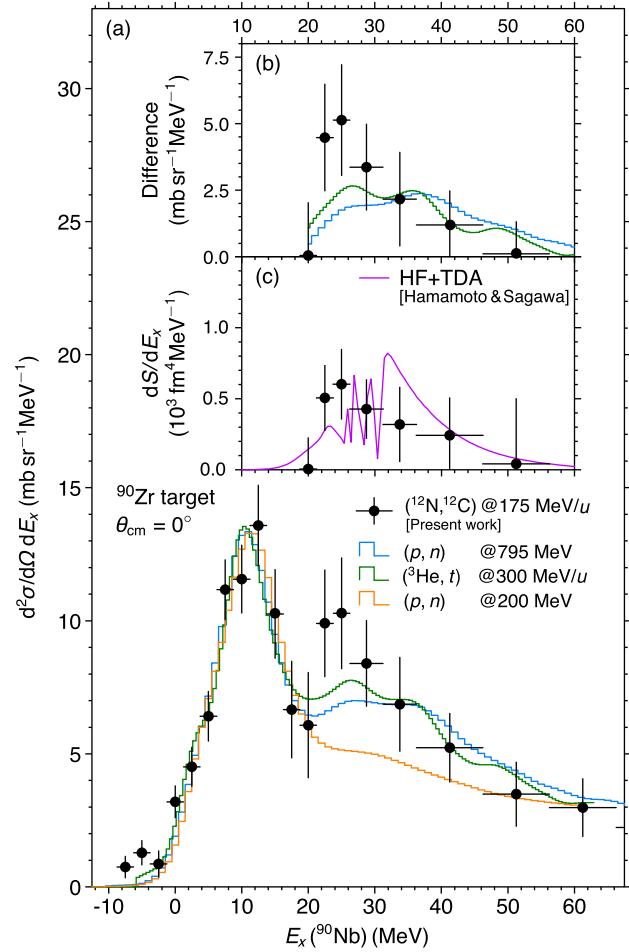


FIG. 3. (a) Comparison of the double-differential cross-section spectra of the present Letter with past experiments [13,14,43]. (b) Differences of the spectra with respect to that of the 200-MeV (*p*, *n*) spectrum [43]. (c) The isovector spin monopole strength distribution in ^{90}Zr from the experimental data compared with theoretical predictions [6].

enhanced because the calculated cross sections drop with increasing momentum transfer *q* and thus E_x . The experimental data exhaust $90 \pm 54\%$ of the NMs-NEWSR. The data are compared with the theoretical strength distribution in the Hartree-Fock (HF) plus Tamm-Dancoff approximation (TDA) using the SGII Skyrme interaction for the IVSMR in ^{90}Zr [6]. The theoretical calculations do reasonably well in describing the data. With the availability of higher beam intensities in the future, more detailed studies in which the monopole strength is extracted through a multipole-decomposition analysis (see, e.g., Ref. [19]) will become possible. Such an analysis would also enable the extraction of the isovector spin dipole strength distribution, expected at $E_x \sim 20$ MeV with a width of $\Gamma \sim 10$ MeV [44], and of other ΔL components. In the present analysis, those contributions are approximately subtracted by using the (*p*, *n*) data at 200 MeV as a reference.

The proportionality [45] between the zero-degree cross section and the GT and Fermi transition strengths, denoted

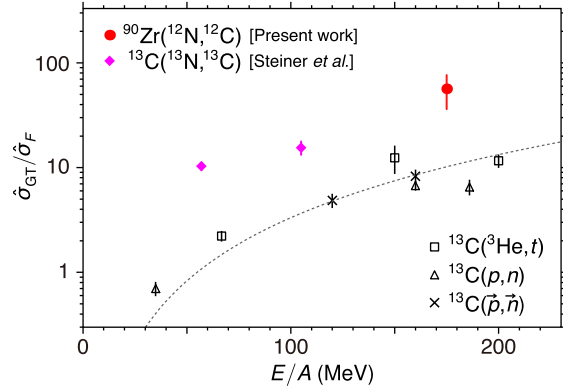


FIG. 4. Ratios of the unit cross sections $\hat{\sigma}_{GT}/\hat{\sigma}_F$ as a function of incident beam energy. The dashed curve shows $\hat{\sigma}_{GT}/\hat{\sigma}_F = [(E/A)/(55 \text{ MeV})]^2$. See text and Ref. [49] for details.

by the unit cross sections $\hat{\sigma}_{GT}$ and $\hat{\sigma}_F$, respectively, have been systematically studied for the $(p, n)/(n, p)$ reactions [46] and for the $(^3\text{He}, t)/(t, ^3\text{He})$ reactions [47,48]. For heavy-ion charge-exchange reactions, similar proportionality exists [49]. By using the measured cross sections from the present Letter in combination with known transition strengths from literature for the $^{12}\text{N} - ^{12}\text{C}$ channel (proj) and the $^{90}\text{Zr} - ^{90}\text{Nb}$ channel (tgt) for GT [$B(\text{GT})_{\text{proj}} = 0.3$, $B(\text{GT})_{\text{tgt}} = 18.3 \pm 3.0$ [43]] and Fermi [$B(F)_{\text{proj}} = 2$, $B(F)_{\text{tgt}} = 10$] transitions, the ratio $\hat{\sigma}_{GT}/\hat{\sigma}_F$ for the $(^{12}\text{N}, ^{12}\text{C})$ probe at 175 MeV/u was determined to be 54 ± 22 .

The ratio is compared with results from Ref. [49] as a function of beam energy in Fig. 4. It is well known that $\hat{\sigma}_{GT}/\hat{\sigma}_F$ strongly increases with beam energy because of the rapid decrease of the τ component of the NN interaction [23,24], and that the ratios for heavier target nuclei are larger (See Ref. [46] and references therein). However, besides these, the value of $\hat{\sigma}_{GT}/\hat{\sigma}_F$ is much higher for the heavy-ion charge-exchange probes, including the present data and the results from the $(^{13}\text{N}, ^{13}\text{C})$ reaction, than for the (p, n) and $(^3\text{He}, t)$ probes. This enhancement can be attributed to the strong absorption of these probes [49]. Since the spin-transfer ($\sigma\tau$) component of the NN interaction has a long range, while the non-spin-transfer (τ) component has a short range [23,24], the latter is strongly reduced when the impact parameters are large, as is the case in heavy-ion charge-exchange reactions. Since the excitation of the IVSMR is also mediated by the $\sigma\tau$ component, this result also gives evidence that the heavy-ion charge-exchange probe is best suitable for studying this giant resonance.

In this Letter, we demonstrated that the $(^{12}\text{N}, ^{12}\text{C})$ reaction at 175 MeV/u is a powerful probe for studying the IVSMR in the β^- direction due to a combination of being exothermic, strongly absorptive, and providing spin selectivity. In the present study, a clear signature of the IVSMR in ^{90}Nb was observed in the region of $E_x = 20\text{--}50$ MeV, besides the well-known GT and Fermi

excitations. A study of the GT and Fermi unit cross section provides further evidence that the $(^{12}\text{N}, ^{12}\text{C})$ reaction is suitable for enhancing the excitations that are mediated by the $\sigma\tau$ interaction, including the IVSMR.

Although the quality of the present data suffered from the limited ^{12}N beam intensity, which made it difficult to perform a detailed multipole decomposition analysis, it has been demonstrated that it will be possible to extract high-quality information about the IVSMR with the availability of more intense beams of ^{12}N in the future.

This experiment was performed at the RI Beam Factory operated by RIKEN Nishina Center and Center for Nuclear Study, University of Tokyo. The authors thank the RIBF and BigRIPS teams for the stable operation of the cyclotrons and the delivery of the secondary beam during the experiment. They are also grateful to Professor Takenori Furumoto for providing the OMP parameters and to Professor Munetake Ichimura for valuable comments. This work was supported by JSPS KAKENHI Grants No. JP17002003, No. JP19204024, and No. JP08J09206. It was also supported by the U.S. National Science Foundation Grants No. PHY-1565546, No. PHY-1068192, and No. PHY-1430152 (JINA Center for the Evolution of the Elements).

*Present address: National Superconducting Cyclotron Laboratory, Michigan State University, East Lansing, Michigan 48824, USA.

noji@nsl.msue.edu

†Present address: Research Center for Nuclear Physics, Osaka University, Ibaraki, Osaka 567-0047, Japan.

‡Present address: Center for Nuclear Study, University of Tokyo, RIKEN Campus, Wako, Saitama 351-0198, Japan.

§Present address: Department of Advanced Energy Engineering Science, Kyushu University, Kasuga, Fukuoka 816-8580, Japan.

||Present address: Facility for Rare Isotope Beams, Michigan State University, East Lansing, Michigan 48824, USA.

¶Present address: Department of Radiation Oncology, Tokyo Women's Medical University, Kawadacho, Shinjuku, Tokyo 162-8666, Japan.

**Present address: Tohoku University, Aoba, Sendai, Miyagi 980-8587, Japan.

††Present address: RIKEN Nishina Center, Hirosawa, Wako, Saitama 351-0198, Japan.

- [1] M. N. Harakeh and A. van der Woude, *Giant Resonances: Fundamental High-Frequency Modes of Nuclear Excitation* (Oxford University Press, New York, 2001).
- [2] N. K. Glendenning, Equation of state from nuclear and astrophysical evidence, *Phys. Rev. C* **37**, 2733 (1988).
- [3] J. M. Lattimer and M. Prakash, Nuclear matter and its role in supernovae, neutron stars and compact object binary mergers, *Phys. Rep.* **333–334**, 121 (2000).
- [4] G. Colò, The compression modes in atomic nuclei and their relevance for the nuclear equation of state, *Phys. Part. Nucl.* **39**, 286 (2008).

- [5] N. Auerbach and A. Klein, Structure of isovector spin excitations in nuclei, *Phys. Rev. C* **30**, 1032 (1984).
- [6] I. Hamamoto and H. Sagawa, Charge-exchange spin monopole modes, *Phys. Rev. C* **62**, 024319 (2000).
- [7] J. D. Bowman, E. Lipparini, and S. Stringari, Isovector monopole excitation energies, *Phys. Lett. B* **197**, 497 (1987).
- [8] P. Danielewicz, P. Singh, and J. Lee, Symmetry energy III: Isovector skins, *Nucl. Phys.* **A958**, 147 (2017).
- [9] B. G. Todd-Rutel and J. Piekarewicz, Neutron-Rich Nuclei and Neutron Stars: A New Accurately Calibrated Interaction for the Study of Neutron-Rich Matter, *Phys. Rev. Lett.* **95**, 122501 (2005).
- [10] B. A. Brown, Neutron Radii in Nuclei and the Neutron Equation of State, *Phys. Rev. Lett.* **85**, 5296 (2000).
- [11] K. Langanke and G. Martínez-Pinedo, Nuclear weakinteraction processes in stars, *Rev. Mod. Phys.* **75**, 819 (2003).
- [12] T. Marketin, G. Martínez-Pinedo, N. Paar, and D. Vretenar, Role of momentum transfer in the quenching of Gamow-Teller strength, *Phys. Rev. C* **85**, 054313 (2012).
- [13] D. L. Prout *et al.*, Observation of the spin isovector monopole resonance using the $\text{Pb}(\bar{p}, \bar{n})\text{Bi}$ reaction at 795 MeV, *Phys. Rev. C* **63**, 014603 (2000).
- [14] A. Brockstedt *et al.*, The $({}^3\text{He}, t)$ reaction at intermediate energies: Spin-isospin multipole transitions, *Nucl. Phys.* **A530**, 571 (1991).
- [15] R. G. T. Zegers *et al.*, Excitation and Decay of the Isovector Giant Monopole Resonances via the ${}^{208}\text{Pb}({}^3\text{He}, tp)$ Reaction at 410 MeV, *Phys. Rev. Lett.* **90**, 202501 (2003).
- [16] R. G. T. Zegers, A. M. van den Berg, S. Brandenburg, M. Fujiwara, J. Guillot, M. N. Harakeh, H. Laurent, S. Y. van der Werf, A. Willis, and H. W. Wilschut, Excitation of the isovector giant monopole resonances via the ${}^{\text{nat}}\text{Pb}({}^3\text{He}, tp)$ reaction, *Phys. Rev. C* **63**, 034613 (2001).
- [17] J. Guillot *et al.*, The $(t, {}^3\text{He})$ reaction at 43 MeV/nucleon on ${}^{48}\text{Ca}$ and ${}^{58}\text{Ni}$: Results and microscopic interpretation, *Phys. Rev. C* **73**, 014616 (2006).
- [18] C. J. Guess *et al.*, The ${}^{150}\text{Nd}({}^3\text{He}, t)$ and ${}^{150}\text{Sm}(t, {}^3\text{He})$ reactions with applications to $\beta\beta$ decay of ${}^{150}\text{Nd}$, *Phys. Rev. C* **83**, 064318 (2011).
- [19] K. Miki *et al.*, Identification of the β^+ Isovector Spin Monopole Resonance via the ${}^{208}\text{Pb}$ and ${}^{90}\text{Zr}(t, {}^3\text{He})$ Reactions at 300 MeV/ u , *Phys. Rev. Lett.* **108**, 262503 (2012).
- [20] N. Auerbach and A. Klein, A microscopic theory of giant electric isovector resonances, *Nucl. Phys.* **A395**, 77 (1983).
- [21] N. Auerbach, F. Osterfeld, and T. Udagawa, The spin isovector monopole strength and the $({}^3\text{He}, t)$ reaction, *Phys. Lett. B* **219**, 184 (1989).
- [22] N. Anantaraman, J. S. Winfield, Sam M. Austin, J. A. Carr, C. Djalali, A. Gillibert, W. Mittig, J. A. Nolen, Jr., and Zhan Wen Long, $({}^{12}\text{C}, {}^{12}\text{B})$ and $({}^{12}\text{C}, {}^{12}\text{N})$ reactions at $E/A = 70$ MeV as spin probes: Calibration and application to 1^+ states in ${}^{56}\text{Mn}$, *Phys. Rev. C* **44**, 398 (1991).
- [23] W. G. Love and M. A. Franey, Effective nucleon-nucleon interaction for scattering at intermediate energies, *Phys. Rev. C* **24**, 1073 (1981); Erratum, *Phys. Rev. C* **27**, 438 (1983).
- [24] M. A. Franey and W. G. Love, Nucleon-nucleon t -matrix interaction for scattering at intermediate energies, *Phys. Rev. C* **31**, 488 (1985).
- [25] M. Ichimura, H. Sakai, and T. Wakasa, Spin-isospin responses via (p, n) and (n, p) reactions, *Prog. Part. Nucl. Phys.* **56**, 446 (2006).
- [26] T. Wakasa *et al.*, Gamow-Teller strength of ${}^{90}\text{Nb}$ in the continuum studied via multipole decomposition analysis of the ${}^{90}\text{Zr}(p, n)$ reaction at 295 MeV, *Phys. Rev. C* **55**, 2909 (1997).
- [27] T. Kubo *et al.*, BigRIPS separator and ZeroDegree spectrometer at RIKEN RI Beam Factory, *Prog. Theor. Exp. Phys.* **2012**, 03C003 (2012).
- [28] T. Kawabata, G. P. A. Berg, T. Kubo, H. Sakai, S. Shimoura, and T. Uesaka, High resolution beam line for the SHARAQ spectrometer, *Nucl. Instrum. Methods Phys. Res., Sect. B* **266**, 4201 (2008).
- [29] H. Miya *et al.*, Development of low-pressure multi-wire drift chambers for high-resolution spectroscopy with radioactive isotope beams, *Nucl. Instrum. Methods Phys. Res., Sect. B* **317**, 701 (2013).
- [30] T. Uesaka, S. Shimoura, and H. Sakai (for the SHARAQ Collaboration), The SHARAQ spectrometer, *Prog. Theor. Exp. Phys.* **2012**, 03C007 (2012).
- [31] S. Takeuchi, T. Motobayashi, Y. Togano, M. Matsushita, N. Aoi, K. Demichi, H. Hasegawa, and H. Murakami, DALI2: A NaI(Tl) detector array for measurements of γ rays from fast nuclei, *Nucl. Instrum. Methods Phys. Res., Sect. A* **763**, 596 (2014).
- [32] M. N. Harakeh, Microscopic structure of charge-exchange spinisospin modes through decay measurements, *Acta Phys. Pol. B* **29**, 2199 (1988).
- [33] F. Ajzenberg-Selove, Energy levels of light nuclei $A = 11-12$, *Nucl. Phys.* **A506**, 1 (1990).
- [34] J. Cook and J. Carr, computer program FOLD/DWHI, Florida State University (unpublished); based on F. Petrovich and D. Stanley, Microscopic interpretation of ${}^7\text{Li} + {}^{24}\text{Mg}$ inelastic scattering at 34 MeV, *Nucl. Phys.* **A275**, 487 (1977); modified as described in J. Cook, K. W. Kemper, P. V. Drumm, L. K. Fifield, M. A. C. Hotchkis, T. R. Ophel, and C. L. Woods, ${}^{16}\text{O}({}^7\text{Li}, {}^7\text{Be}){}^{16}\text{N}$ reaction at 50 MeV, *Phys. Rev. C* **30**, 1538 (1984); R. G. T. Zegers, S. Fracasso, and G. Colò (unpublished).
- [35] T. Suzuki, R. Fujimoto, and T. Otsuka, Gamow-Teller transitions and magnetic properties of nuclei and shell evolution, *Phys. Rev. C* **67**, 044302 (2003).
- [36] B. A. Brown, W. D. M. Rae, E. McDonald, and M. Horoi, NuSHELLX@MSU, <http://www.nscl.msu.edu/~brown/resources/resources.html>.
- [37] S. Y. van der Werf, computer program NORMOD (unpublished).
- [38] T. Furumoto, Y. Sakuragi, and Y. Yamamoto, New complex G -matrix interactions derived from two- and three-body forces and application to proton-nucleus elastic scattering, *Phys. Rev. C* **78**, 044610 (2008).
- [39] T. Furumoto, Y. Sakuragi, and Y. Yamamoto, Three-body-force effect on nucleus-nucleus elastic scattering, *Phys. Rev. C* **79**, 011601(R) (2009).
- [40] T. Furumoto, Y. Sakuragi, and Y. Yamamoto, Effect of repulsive and attractive three-body forces on

- nucleus-nucleus elastic scattering, *Phys. Rev. C* **80**, 044614 (2009). Erratum, *Phys. Rev. C* **82**, 029908 (2010).
- [41] T. Furumoto, Y. Sakuragi, and Y. Yamamoto, Repulsive nature of optical potentials for high-energy heavy-ion scattering, *Phys. Rev. C* **82**, 044612 (2010).
- [42] L. C. Chamon, B. V. Carlson, L. R. Gasques, D. Pereira, C. De Conti, M. A. G. Alvarez, M. S. Hussein, M. A. Cândido Ribeiro, E. S. Rossi, Jr., and C. P. Silva, Toward a global description of the nucleus-nucleus interaction, *Phys. Rev. C* **66**, 014610 (2002).
- [43] C. Gaarde, Gamow-Teller and $M1$ resonances, *Nucl. Phys.* **A396**, 127 (1983).
- [44] K. Yako, H. Sagawa, and H. Sakai, Neutron skin thickness of ^{90}Zr determined by charge exchange reactions, *Phys. Rev. C* **74**, 051303(R) (2006).
- [45] T. N. Taddeucci, C. A. Goulding, T. A. Carey, R. C. Byrd, C. D. Goodman, C. Gaarde, J. Larsen, D. Horen, J. Rapaport, and E. Sugarbaker, The (p, n) reaction as a probe of beta decay strength, *Nucl. Phys.* **A469**, 125 (1987).
- [46] M. Sasano *et al.*, Gamow-Teller unit cross sections of the (p, n) reaction at 198 and 297 MeV on medium-heavy nuclei, *Phys. Rev. C* **79**, 024602 (2009).
- [47] R. G. T. Zegers *et al.*, Extraction of Weak Transition Strengths via the $(^3\text{He}, t)$ Reaction at 420 MeV, *Phys. Rev. Lett.* **99**, 202501 (2007).
- [48] G. Perdikakis *et al.*, Gamow-Teller unit cross sections for $(t, ^3\text{He})$ and $(^3\text{He}, t)$ reactions, *Phys. Rev. C* **83**, 054614 (2011).
- [49] M. Steiner *et al.*, First Study of Heavy-Ion Mirror Charge Exchange, *Phys. Rev. Lett.* **76**, 26 (1996). Erratum, *Phys. Rev. Lett.* **76**, 3042 (1996).